Identifying the Kinematic Parameters of Hexapod Machine Tool

M. M. Agheli, M. J. Nategh

Abstract—Hexapod Machine Tool (HMT) is a parallel robot mostly based on Stewart platform. Identification of kinematic parameters of HMT is an important step of calibration procedure. In this paper an algorithm is presented for identifying the kinematic parameters of HMT using inverse kinematics error model. Based on this algorithm, the calibration procedure is simulated. Measurement configurations with maximum observability are decided as the first step of this algorithm for a robust calibration. The errors occurring in various configurations are illustrated graphically. It has been shown that the boundaries of the workspace should be searched for the maximum observability of errors. The importance of using configurations with sufficient observability in calibrating hexapod machine tools is verified by trial calibration with two different groups of randomly selected configurations. One group is selected to have sufficient observability and the other is in disregard of the observability criterion. Simulation results confirm the validity of the proposed identification algorithm.

Keywords—Calibration, Hexapod Machine Tool (HMT), Inverse Kinematics Error Model, Observability, Parallel Robot, Parameter Identification.

I. INTRODUCTION

HEXAPOD machine tool (HMT) is a parallel robot based on Stewart platform. HMT calibration similar to calibration of other serial and parallel manipulators encompasses four essential tasks, as follows: modeling, measurement, parameter identification and implementation or compensation [1]-[4].

The First step in the calibration of any type of robots is modeling. For kinematic calibration, a kinematics model of the robot is needed. Measurement of the position and orientation of the moving platform is the second and an important step in robot calibration [5]. The best results for robot calibration are obtained when the proper measurement configurations are selected [2], [6]-[13]. For this purpose the kinematics parameters errors must be observable and identifiable in the selected configurations.

Kinematics parameters errors of parallel robots have been investigated by some researchers: Jokiel and Zigert [9] have worked on errors of hexapod. Ridgeway and Crane [14] have

M. M. Agheli is with the Engineering Faculty, Mechanical Engineering Department, Tarbiat Modares University, Tehran, Iran.

M. J. Nategh is with the Engineering Faculty, Mechanical Engineering Department, Tarbiat Modares University, Tehran, Iran (phone: +98-21-82884396; e-mail: nategh@ modares.ac.ir).

proposed an approach for optimization of parallel systems kinematics considering position and orientation errors. Szatmari [15] has presented some proposals about the identification and creation of graphics of geometrical errors occurring in a parallel manipulator. Also error of parallel mechanisms based on Stewart platform has been studied by a number of researchers. For more details, readers are referred to [4] and [16]-[26].

The third step of a calibration procedure is parameter identification. The real or fairly real values of kinematic parameters which are needed for calibration procedure are identified in the parameter identification step. This step is done on the basis of the configurations which are selected for measurement called the measurement configurations. The accuracy of the kinematic parameters depends on the degree of observability of the measurement configurations, i. e. more accurate parameters are obtained with more observable measurement configurations.

An algorithm is proposed in this paper for identifying the kinematic parameters of HMT. This algorithm can also be applied to other kinds of serial and parallel robots. A graphical representation of the error has also been employed to determine the maximum observability of the kinematic parameter errors within the robot workspace. Based on this graphical model, the configurations with the utmost observability are selected. The calibration is then simulated based on the proposed algorithm and the selected configurations.

II. MODELING THE HMT

HMT is a parallel manipulator that consists of six variable-length legs (l_i) connected at one end to a fixed base by U-joints (universal joint) and at the other end to a moving platform by S-joints (spherical joint). This mechanism is shown in Fig.1.

A global coordinate system, $\{O\}$, is defined with its centre point coincident with the centre of the stationary platform. A local coordinate system, $\{C\}$, is also defined with its centre point coincident with the centre of the moving platform namely and respectively. The vector of the centre of the U-joints on the fixed base are denoted by $\vec{u}_i$, $i = 1,2,...,6$ in the global coordinates and the vector of the centre of the S-joints on the moving platform are denoted by $\vec{s}_i$, $i = 1,2,...,6$ in the local coordinates.
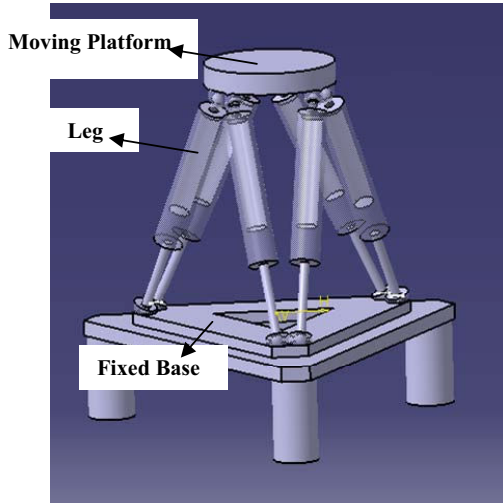
Fig. 1 Hexapod Machine Tool

The orientation and the position of the moving platform are denoted by R and $\vec{o} = [x \quad y \quad z]^T$ with respect to the global coordinates $\{O\}$, respectively. R is the 3×3 rotation matrix and $\vec{o}$ is a 3×1 vector. The details are shown in Fig.2.
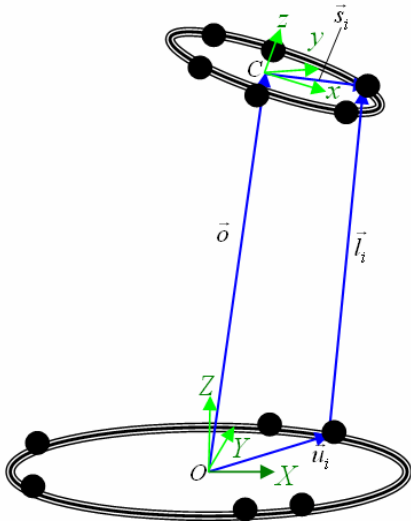
Fig. 2   The vector representation of the ith leg's kinematic chain

The inverse kinematics finds the leg lengths based on given orientation and position of the moving platform whereas the forward kinematics finds the orientation and the position of the moving platform based on the given leg lengths. The vectors $\vec{u}_i$ and $\vec{s}_i$ are theoretically invariables for both the inverse and the forward kinematics.

From Fig.2 illustrating the closed kinematic chain of ith leg, the inverse kinematics of HMT can be expressed as follows:

$$\vec{l}_i = \vec{o} + R\vec{s}_i - \vec{u}_i \tag{1}$$

By using the inverse kinematics model, the error of the moving platform can be illustrated in the workspace based on the kinematics parameters error. This is done in section IV.

III.   IDENTIFICATION ALGORITHM

The major purpose of the calibration procedure is identification of the real or near real values of the kinematics parameters. For this purpose, an identification algorithm is proposed as in Fig.3.
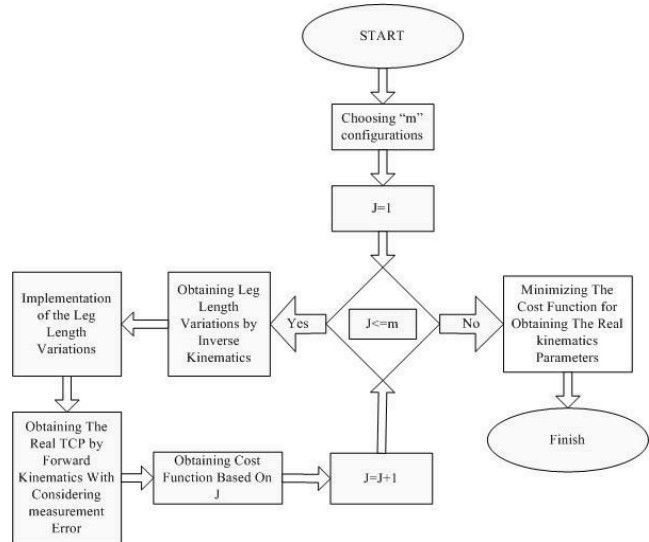

Fig. 3 Identification Algorithm

This algorithm encompasses six major steps:

Step 1: Choosing "m" configurations; fifteen configurations are selected on the basis of the degree of observability being discussed in the next section.

Step 2: Inverse kinematics solution; for each of the 15 configurations, the inverse kinematics is solved and the leg lengths are calculated each configuration.

Step 3: if the initial leg length (offset) is deducted from the calculated leg length, the leg length variation that should be implemented to achieve the calculated leg length is obtained. This leg length variation must be applied to the initial leg length.

Step 4: Measuring the poses; by applying the leg length variation to the initial leg length, it is anticipated theoretically that desired position and orientation of the platform is achieved. But because of the existence of various error sources such as manufacturing and assembly errors the desired orientation and position cannot be achieved. That is why the calibration procedure is essential. In simulation procedure, obtaining the difference between the occurred pose and desired pose is very important. It is discussed in simulation section.

Step 5: by replacing the measurement data in the cost function for each configuration and repeating it for all the "m" configurations, the cost function is obtained.

Step 6: minimizing the cost function for achieving the real values of the kinematics parameters is the last step of the identification algorithm.

After replacing the identified kinematicss parameters for controller instead of the nominal values, the calibration procedure is complete.

According to the identification algorithm, the first step is determining the *m* measurement.

IV. OBSERVABILITY AND CONFIGURATION SELECTION

Some parts of the robot workspace have more observability of the kinematic parameter errors than the other parts. It means that in these parts of workspace, the kinematics parameters errors have more influence on the platform error than the other parts. For detecting these parts of the robot workspace, in this section the effect of the kinematics parameter errors within the workspace has been obtained graphically. For this purpose, after obtaining the error model, by imparting a range of error to the kinematics parameters, platform pose error has been illustrated. A random range of the kinematics parameters error between -0.1mm and $+0.1$mm is assumed. The results for the position and orientation error of the platform are illustrated graphically as in Fig.4 for x direction and in Fig.5 for y direction. Hundred diagrams have been obtained for 100 different values of z. All these diagrams yielded similar results being discussed below. However, just twenty of these diagrams are illustrated in the figure to avoid any ambiguity.
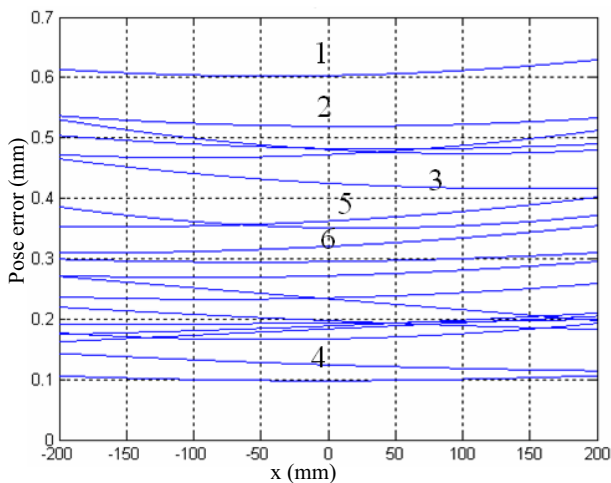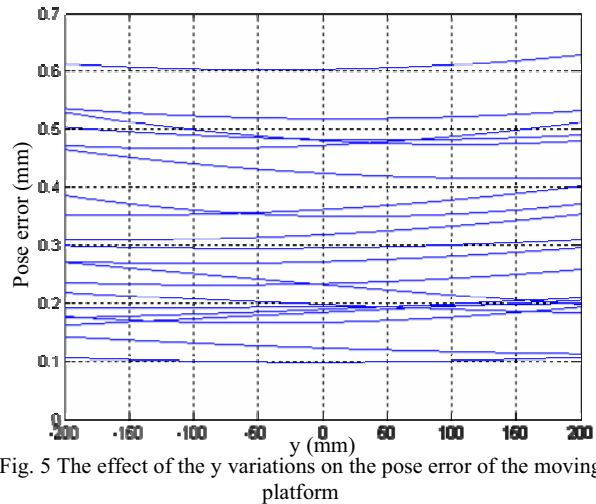

Fig. 5 The effect of the y variations on the pose error of the moving platform

All the above results indicate that the maximum error of the upper platform's pose due to the kinematics parameters errors occurs in the workspace boundary. It means that the observability of the kinematics parameters errors in the boundary of the workspace is more than the other parts of workspace. This is also the case for z direction as illustrated in Fig.6.
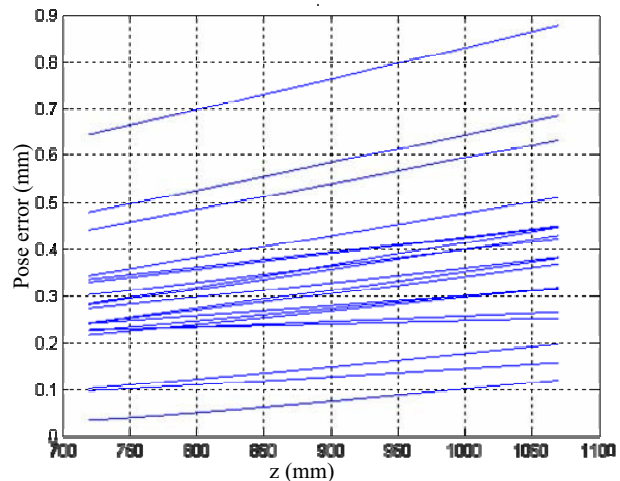

Fig. 4 The effect of the x variations on the pose error of the moving platform

Fig. 6 The effect of the z variations on the pose error of the moving platform

The curves in Figs. 4 and 5 can be divided into three categories, as follows: 1) the curves such as curves number 1 and 2 imply that the maximum error of the moving platform's pose due to the kinematics parameters errors occurs in both ends of the cures (right and left sides); 2) the curves such as curves number 3 and 4 imply that the maximum error of the moving platform's pose due to the kinematics parameters errors occurs only in the left ends of the curves; 3) the curves such as curves number 5 and 6 indicate that the maximum error of moving platform's pose due to the kinematics parameters errors occurs only in right end of the curve.

It is obvious from Fig. 6 that better observability exists at higher levels of the moving platform along z axis. In other words, maximum observability is obtained at larger z values. A similar argument can also be presented for the angular boundaries of the workspace. The upper platform's pose error against the variations of a, b, and c are illustrated in Figs. 6-8. The values of a, b, and c are the angles of the upper platform around x, y and z axes, respectively.
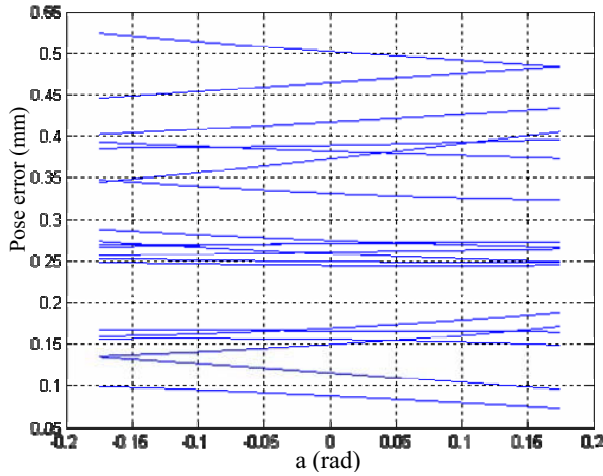
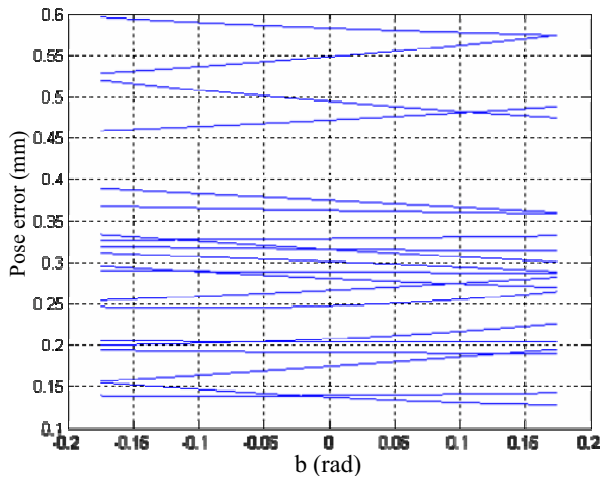Fig. 7 The effect of variations of a and b on the pose error of the upper platform

Fig. 8 The effect of variations of a and c on the pose error of the upper platform

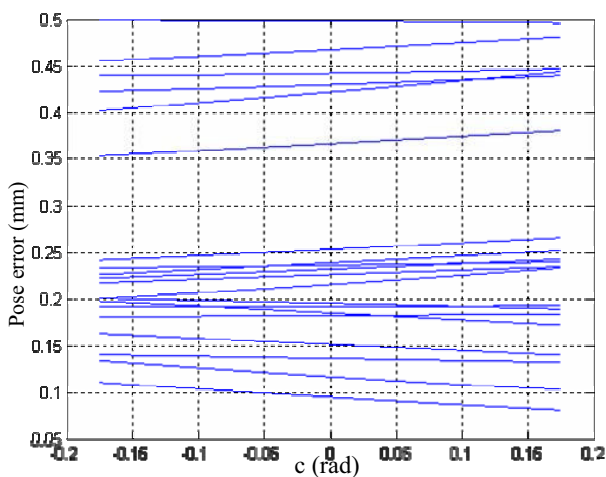
Fig. 9 The effect of variations of b and c on the pose error of the upper platform

Fi.g 7 shows the upper platform's pose error against variations of a for constant values of b and c. The pose error against variations of b for constant values of a and c is shown in Fi. 8. The pose error against variations of c for constant values of a and b is shown in Fi. 8.

Figs. 7-9 indicate that higher observability of the kinematics parameters errors is achieved at extreme angular boundaries of the workspace. Therefore, the maximum observability of kinematics parameters errors should be searched for at the boundaries of the workspace with the maximum angle of the orientation of the moving platform. In other words, the measurement configurations should be selected on the boundary of the workspace.

For each x, y, z, a, b, and c parameters, two levels are selected; one for the maximum positive direction and the second for the maximum negative direction. Therefore, there are 64 (2^6) configurations on the boundary of the workspace as candidates for measurement configurations with maximum observability. From among these 64 configurations, 15 configurations are randomly selected. It is obvious that these 15 configurations have more observability than the other configurations within the HMT workspace but are not situated on the boundary of the workspace.

V. COST FUNCTION

The inverse kinematics can be rewritten from (1), as follows:

$$\left\| \vec{o} + R\vec{s}_i - \vec{u}_i \right\| = \left\| \vec{l}_i \right\| = l_i \qquad (2)$$

where $l_i = l_{oi} + \Delta l_i$ is the ith leg's length as the sum of the initial leg's length (l_{oi}) and the leg's length variations (Δl_i). The cost function, defined at all measurement configurations, is derived as follows [3]:

$$CF = \sum_{j=1}^{m} \sum_{i=1}^{6} [(\vec{o}_j + R_j\vec{s}_i - \vec{u}_i)^T (\vec{o}_j + R_j\vec{s}_i - \vec{u}_i) - (l_{oi} + \Delta l_{i,j})^2]^2 \qquad (3)$$

where $(\vec{o}_j + R_j\vec{s}_i - \vec{u}_i)^T (\vec{o}_j + R_j\vec{s}_i - \vec{u}_i) = \left\| \vec{o}_j + R_j\vec{s}_i - \vec{u}_i \right\|^2$ is the square of the norm of the leg's length computed from inverse kinematics at pose j; m is the number of the selected configurations. For the actual kinematics parameters of the robot, the general cost function should be approximately zero. Therefore the general cost function must be minimized. The least square approach based on Levenberg-Marquardt algorithm is used to minimize this function. Minimizing this function gives the real values or near real values of the kinematics parameters.

VI. SIMULATION

Calibration procedure is simulated throughout these 15 configurations. Also it is simulated for 15 other random configurations inside the workspace but not on the workspace boundary (step 1).

The leg length variation is calculated by solving the inverse kinematics equation in each configuration (steps 2 and 3).

Real kinematics parameters are assumed with a random error in range of $-5\text{mm} \leq error \leq +5\text{mm}$ as compared to the nominal values of kinematics parameters. For each configuration, real position and orientation of the moving platform is calculated by solving the forward kinematics problem based on the assumed real kinematics parameters and the assumed error for leg length measurement device occurring within $-0.01\text{mm} \leq error \leq +0.01\text{mm}$. A random measurement noise in range of $-0.025\text{mm} \leq error \leq +0.025\text{mm}$ for position error of the measurement device and $-0.001\text{rad} \leq error \leq +0.001\text{rad}$ for orientation error of measurement device is propagated to the calculated position and orientation (step 4).

A least square method based on Levenberg-Marquardt algorithm is implemented to solve the cost function obtained by difference between calculated and measured leg lengths (steps 5 and 6).

Simulation results for identified kinematics parameters are illustrated in Fig.10.
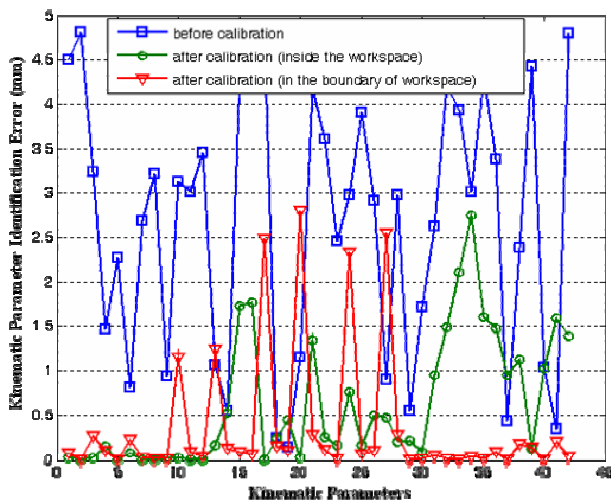

Fig. 10 Simulation results of identification

These results are shown in Table I. Results show the validity of the identification algorithm and selected configurations. Identification error is reduced about 50 percent when the configurations are select on the boundary of the workspace.

TABLE 1 ERROR OF IDENTIFIED KINEMATICS PARAMETERS

Kinematics Parameters Errors	Before calibration	After calibration (15 configurations inside the workspace)	After calibration (15 configurations on the boundary)
Mean (mm)	2.6652	0.7236	0.3752

By using the values obtained from the simulation results, positioning of the platform is done for 10 other configurations within the 49 (= 64-15) remaining configurations in which the observability is maximum, to verify the validity of the proposed identification algorithm and chosen measurement configurations. Position and orientation error in these configurations after calibration is shown in Fig. 11. The error having occurred in the position and the orientation of the platform before calibration was around 15mm and .05rad, respectively.
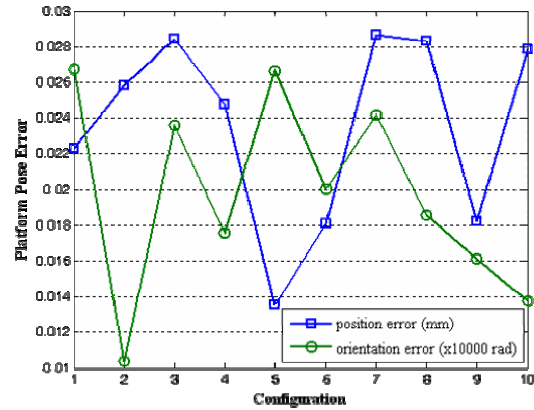

Fig. 11 Simulation results for position and orientation errors of the moving platform after calibration

Comparison between the results before and after calibration shows that the position and orientation error have been reduced around 500 times and 15000 times, respectively.

VII. CONCLUSION

An Identification algorithm was proposed to identify the real or near real kinematics parameters. Calibration of a hexapod machine tool was simulated according to this algorithm.

It was verified in the present study that boundary configurations of the hexapod machine tools delivered maximum observabilty of the kinematics errors for the purpose of calibration. Moreover, as far as the height of the moving platform was concerned, maximum observability was achieved when the platform was situated at its highest level.

Simulation results indicated that hexapod machine tool could be positioned with an error less than 0.03mm and could be oriented with an error less than 0.000003 rad. These values confirmed the validity of the proposed identification algorithm.

REFERENCES

[1] Benjamin W.Mooring and Zvi S. Roth and Morris R. Driels, "Fundamentals of Manipulator Calibration", John Wiely & Sons, New York, 1991.

[2] H. Zhuang, Y. Jiahua, and O. Masory, "Calibration of Stewart platforms and other parallel   manipulators by minimizing inverse kinematics residuals," Journal of Robotic Systems, vol. 15, pp. 395–405, 1998.

[3] Yu-jen Chiu,Ming-Hwei Perng, "Self-calibration of a general hexapod manipulator with enhanced precision in 5-DOF motions", Mechanism and Machine Theory, vol. pp. 1-23, 2004.

[4] K. T. Sung, W. Park, and Y K. Lee, "Study on Observability of Parallel-typed Machining Centre Using a Single Planar Table and Digital Indicators," *Mechanism and Machine Theory*, vol. 41, pp. 1147-1156, 2006.

[5] H. Zhuang, K. Wang, and Z. S. Roth, "Optimal selection of measurement Configurations for robot calibration using simulated

annealing," *Proceedings of the IEEE International Conference on Robotics and Automation (ICRA)*, San Diego, CA, pp. 393–398, 1994.

[6] T,Anderson, M.J.Thurley, O.Marklund, "Pellet Size Estimation Using Spherical Fitting", *Instrumentation and Measurement Technology Conference Proceedings IEEE*, Location: Warsaw, ISSN: 1091-5281, ISBN: 1-4244-0588-, pp. 1-5, 2007.

[7] David Daney, Ioannis Z. Emiris, "Calibration of parallel robots : on the Elimination of Pose–Dependent Parameters", Proceedings of EUCOMES, the first European Conference on Mechanism Science , Obergurgl (Austria), February 21–26, 2006.

[8] David Daney, Yves Papegay, "Choosing Measurement Poses for Robot Calibration with the Local Convergence Method andTabu Search", International Journal of Robotic Research, Sage publications, vol. 24, pp. 501-518, 2005.

[9] Bernhard Jokiel Jr. , John C. Ziegert , and Lothar Bieg, "Uncertainty propagation in calibration of parallel kinematics machines," *Precision Engineering*, vol. 25, pp. 48-55, 2001.

[10] A. Nahvi, J. M. Hollerbach, and V. Hayward, "Calibration of a parallel robot using multiple kinematics closed loops," *Proceedings of the IEEE International Conference on Robotics and Automation (ICRA),* San Diego, CA, pp. 407–412, 1994.

[11] A. Nahvi, and J. M. Hollerbach, "The noise amplification index for optimal pose selection in robot calibration," *Proceedings of the IEEE International Conference on Robotics and Automation (ICRA),* Minneapolis, MN, pp. 647–654, 1996.

[12] J. H. Borm, and C. H. Menq, "Determination of optimal measurement Configurations for robot calibration based on observabililty measure," *Journal of Robotic Systems* , vol. 10, pp. 51–63, 1991.

[13] C.H. Meng, J.H. Borm, "Identification and observability measure of a basis set of error parameters in robot calibration", *J. Mechanism, Transmissions and automation in design*, vol. 111, pp. 513-518, 1989.

[14] Shannon C. Ridgeway , Carl D. Crane , "Optimized Kinematics of a 6-6 Parallel Mechanism Considering Position and Orientation Errors", FCRAR 2003, The 16th Florida Conference on the Recent Advances in Robotics, Florida Atlantic University, Boca Raton, FL, May 2003.

[15] szabolcs szatmári , "geometrical errors of parallel robots", *periodica polytechnica ser. mech. eng.*, vol. 43, no. 2, pp. 155–162, 1999.

[16] GAO Meng, LI Tiemin, TANG Xiaoqiang, DUAN Guanghong, "Estimates of Identification Result Disturbances in Parallel Mechanism Calibration", *Tsinghua Science and Technology* , vol. 11, pp. 80-87, 2006.

[17] Hai Wang, Kuang-Chao Fan ," Identification of strut and assembly errors of a 3- PRS serial–parallel machine tool", *International Journal of Machine Tools & Manufacture*, vol. 44, pp. 1171–1178, 2004.

[18] Han Sung Kim, "Kinematics Calibration of a Cartesian Parallel Manipulator", *International Journal of Control, Automation, and Systems*, vol. 3, pp. 453-460, 2005.

[19] Yung Ting , Ho-Chin Jar, Chun-Chung Li, "Measurement and calibration for Stewart micromanipulation system", *Precision Engineering*, vol., pp. 226-233, 2007.

[20] Haomin Lin, John E. McInroy, "Disturbance attenuation in precise hexapod pointing using positive force feedback", *Control Engineering Practice*, vol. 14, pp. 1377–1386, 2006.

[21] Rocco Vertechy, Vincenzo Parenti Castelli, " Accurate and fast body pose estimation by three point position data," Mechanism and machine theory, vol. 42, pp.1170-1183, 2007.

[22] Tae-Young Lee, Jae-Kyung Shim, "Improved dialytic elimination algorithm for the forward kinematics of the general Stewart–Gough platform", *Mechanism and Machine Theory*, vol. 38, 563–577, 2003.

[23] E. Castillo-Castaneda, Y. Takeda, "Improving path accuracy of a crank-type 6-dof parallel mechanism by stiction compensation", *Mechanism and Machine Theory*, vol. 43, pp.104-114, 2008.

[24] J. Gao, P. Webb and N. Gindy, "Error reduction for an inertial-sensor-based dynamic parallel kinematics machine positioning system", *Meas. Sci. Technol.*, vol. 14, pp. 543-550, 2003.

[25] Takaaki OIWA, "Study on Accuracy Improvement of Parallel Kinematics Machine-Compensation Methods for Thermal Expansion of Link and Machine Frame-", *1st Korea Japan Conf Positioning Technol*, pp. 189-194, 2002.

[26] Seung Reung Lim, Woo Chun Choi, Jae-Bok Song and Daehie Hong, "Error Model and Accuracy Analysis of a Cubic Parallel Device", *International Journal of the Korean Society of Precision Engineering*, vol. 2, 2001.